International Journal of Pharmaceutics 441 (2013) 56–66

Contents lists available at SciVerse ScienceDirect

International Journal of Pharmaceutics

journal homepage: www.elsevier.com/locate/ijpharm

Pharmaceutical nanotechnology

Formulation optimization and topical delivery of quercetin from solid lipid based nanosystems

Sonali Bose[a,b], Yuechao Du[c], Paul Takhistov[c], Bozena Michniak-Kohn[a,*]

[a] Ernest Mario School of Pharmacy, Rutgers, The State University of New Jersey, 160 Frelinghuysen Road, Piscataway, NJ 08854, USA
[b] Pharmaceutical and Analytical Development, Novartis Pharmaceuticals Corporation, One Health Plaza, East Hanover, NJ 07936, USA
[c] Department of Food Science, Rutgers, The State University of New Jersey, New Brunswick, NJ 08901, USA

ARTICLE INFO

Article history:
Received 18 June 2012
Received in revised form
28 November 2012
Accepted 12 December 2012
Available online 20 December 2012

Keywords:
Sonication
Glyceryl behenate
Solid lipid nanoparticles
Physical stability
Tween 20
Ionic stabilizer

ABSTRACT

The presence of large amounts of reactive oxygen species (ROS) leads to oxidative stress that can damage cell membranes, lead to DNA breakage and cause inactivation of free radical scavenger enzymes, eventually resulting in skin damage. Quercetin is a natural flavonoid that has been shown to have the highest anti-radical activity, along with the ability to act as a scavenger of free radicals and an inhibitor of lipid peroxidation. In this research work, a solvent-free solid lipid based nanosystem has been developed and evaluated for topical delivery of quercetin. Systematic screening of the formulation and process parameters led to the development of a solid lipid (glyceryl dibehenate) based nanosystem using a probe ultrasonication method. The selected variant demonstrated good physical stability for up to 8 weeks at 2–8 °C. Transmission electron microscopy (TEM) images showed spherical particles in the nanometer range. *In vitro* release studies showed biphasic release of quercetin from the SLN formulation, with an initial burst release followed by prolonged release for up to 24 h. *In vitro* permeation studies using full thickness human skin showed higher amounts of quercetin to be localized within the skin compared to a control formulation with particles in the micrometer range. Such accumulation of quercetin in the skin is highly desirable since the efficacy of quercetin in delaying ultra-violet radiation mediated cell damage and eventual necrosis mainly occurs in the epidermis.

1. Introduction

Quercetin (3,3′,4′,5,7-pentahydroxyflavone) is classified as a flavonol, a sub-class of flavonoids, that is commonly found in the plant kingdom. It is present in numerous edible fruits and vegetables such as onions, apples, berries and red grapes. Quercetin has been shown to promote a wide range of pharmacological activities related to the anti-oxidant systems of the skin, including the scavenging of oxygen radicals (Bors et al., 1990, 1994), protection against lipid peroxidation (Laughton et al., 1991) by reducing the amount of malondialdehyde (Erden Inal et al., 2001) and complexation of transition metal ions to form inert chelate complexes (Afanas'ev et al., 1989; Cao et al., 1997). In a comparative study of three flavonoids, catechin, quercetin and diosmetin, quercetin was shown to exhibit a higher antiradical activity toward hydroxyl radicals, peroxyl anions and superoxide anions due to the presence of three active functional groups in its structure (Morel et al., 1993). The expression of matrix metalloproteinase-1, responsible for skin wrinkling and loss of elasticity in both healthy and photoaged skin, has also been observed to be reduced by quercetin at both the mRNA and protein levels (Sim et al., 2007). In addition, quercetin has been shown to be a potent inhibitor of UVB-induced oxidative skin damage following topical application to the skin (Casagrande et al., 2006; Gonzalez et al., 2008). These facts coupled with its safety profile and its natural origin make quercetin a very attractive candidate for incorporation into formulations intended for topical delivery to the skin.

The aqueous solubility of quercetin has been reported to be as low as 0.55 μM (Azuma et al., 2002) with an octanol–water partition coefficient (log *P*) around 1.82 ± 0.32 (Rothwell et al., 2005). Although the log *P* of quercetin is theoretically adequate to permeate the skin, its rather limited solubility in water is believed to hinder permeation through the skin and limit bioavailability (Bonina et al., 1996). This has been confirmed by *in vitro* skin permeation studies where limited permeation of quercetin through the stratum corneum into the deeper layers of the skin has been reported (Kitagawa et al., 2009; Tan et al., 2011).

Various strategies have been attempted to improve the permeability of quercetin through the skin to facilitate topical/transdermal delivery. These include the use of permeation

* Corresponding author. Current address: Department of Pharmaceutics, 160 Frelinghuysen Road, Piscataway, NJ 08854, USA. Tel.: +1 732 445 3589; fax: +1 732 445 5006.
E-mail address: michniak@biology.rutgers.edu (B. Michniak-Kohn).

0378-5173/$ – see front matter © 2013 Elsevier B.V. All rights reserved.
http://dx.doi.org/10.1016/j.ijpharm.2012.12.013

enhancers like dimethylformamide and L-menthol (Olivella et al., 2007), synthesis of ester prodrugs of quercetin (Montenegro et al., 2007), microemulsion based approaches (Censi et al., 2012; Vicentini et al., 2008) and the use of lecithin–chitosan nanoparticles (Tan et al., 2011). Most of these studies have shown some degree of quercetin permeation into the skin but no transdermal delivery. In an *in vitro* study using a Transcutol® P based microemulsion, about 0.9% of the administered dose of quercetin was detected in the receptor compartment of a Franz diffusion cell after 12 h (Censi et al., 2012). The enhancement in quercetin permeation through the skin was attributed to the ability of Transcutol® P to easily permeate the skin thereby facilitating the diffusion of the solubilized quercetin.

Occlusion of the skin surface leads to an increased hydration of the stratum corneum and reduction in the packing of corneocytes, thereby facilitating drug penetration into the deeper layers of the skin (Cevc, 2004; Zhai and Maibach, 2001). These occlusive effects have been reported to be related to the particle size, with nanoparticles (~200 nm) showing 15 times higher occlusivity than microparticles (~4 μm) (Wissing et al., 2001). Lipid based nanosystems that have been investigated for topical applications include solid lipid nanoparticles (SLN), nanostructured lipid carriers (NLC) and nanoemulsions (NE) (Schafer-Korting et al., 2007). SLN are composed of lipids that are solid at ambient temperature whereas NLC are mixtures of solid and liquid lipids. Some of the advantages of SLN and NLC include the use of physiological lipids in the composition, the avoidance of organic solvents, the possibility to produce concentrated lipid suspensions and the availability of established scale-up processes (Mehnert and Mader, 2001). Topical application of SLN and NLC based systems have been studied with various active compounds such as Vitamin E (Dingler et al., 1999), Vitamin A (Jenning et al., 2000a), clotrimazole (Souto et al., 2004), triptolide (Mei et al., 2003), retinoic acid (Castro et al., 2009) and tretinoin (Shah et al., 2007).

SLNs containing quercetin have been previously evaluated for oral delivery (Li et al., 2009) and brain delivery (Dhawan et al., 2011). Recently, nanostructured lipid carriers of quercetin have been developed using a solvent (chloroform/acetone) based emulsification technique and evaluated for topical delivery (Chen-yu et al., 2012). One of the major disadvantages of a manufacturing method involving the use of organic solvents can be toxicological issues arising from solvent residues. The aim of our study was to develop a solvent free solid lipid based nanosystem of quercetin using a probe ultrasonication process. The beneficial pharmacological action of quercetin on the skin coupled with the various advantages of SLN and NLC systems in delivering drugs topically make such a system very attractive. Compritol® 888 and Precirol® ATO 5 were selected as the solid lipids and various non-ionic and anionic surfactants were evaluated to determine their effect on SLN stability. Systematic screening of the formulations and process parameters were carried out for the development of a physically and chemically stable nanosystem. Characterization of the systems was performed and included particle size, zeta potential, morphology, crystallinity, physical stability, *in vitro* release rates of quercetin and evaluation of the formulation as a topical delivery system using full thickness human skin. All excipients evaluated in this study were deemed as safe for human use in skin delivery systems.

2. Materials and methods

2.1. Materials

Highly pure (>99%) quercetin was obtained from Merck (Darmstadt, Germany). Compritol® 888 (glyceryl dibehenate) and Precirol® ATO 5 (glyceryl palmitostearate) were donated by Gattefossé (Paramus, NJ, USA). Poloxamer 188 and sodium lauryl sulfate (SLS) were purchased from BASF (Florham Park, NJ, USA) and TensaChem S.A. (Ougree, Belgium) respectively. Tween 20 (polyoxyethylene derivative of sorbitan monolaurate), Tween 80 (polyoxyethylene derivative of sorbitan monooleate) and dioctyl sodium sulfosuccinate (DOSS) were purchased from Sigma–Aldrich Corporation (St. Louis, MO, USA). All other solvents and reagents used were of HPLC or analytical grade.

2.2. Surface tension measurement of surfactants

The surface tension of various non-ionic (Poloxamer 188, Tween 20 and Tween 80) and anionic (sodium lauryl sulfate (SLS) and dioctyl sodium sulfosuccinate (DOSS)) surfactants in deionized water were measured using the pendant drop method (Semmler and Kohler, 1999) on a contact angle goniometer (Ramé-Hart Instrument Co., Succasunna, NJ, USA). This method measures the profile of a drop hanging at the tip of a capillary. The instrument uses a proprietary edge tracing technology to precisely capture and analyze the drop dimensions and profile characteristics in order to accurately calculate the surface tension of the liquid using the Young–Laplace equation. All measurements were performed in triplicate at 25 °C.

2.3. Preparation of lipid nanoparticles

Quercetin nanoparticles were prepared using the probe ultrasonication method, which has been used previously for the production of lipid nanoparticles (Delmas et al., 2011). 0.5 g of Compritol® 888 ATO (glyceryl dibehenate) or Precirol® ATO 5 (glyceryl palmitostearate) either alone or in combination (3:2 ratio of compritol:precirol) with 0.025 g of quercetin was melted at 85 °C using a water bath. The heated mixture of solid lipid and quercetin was then mixed using sonication with 20 mL of pre-heated surfactant solution (compositions discussed in subsequent sections) at a specific speed for a pre-determined time interval (speed and sonication times described in subsequent section) at 85 °C using a Sonic Dismembrator Model 550 (Fisher Scientific, Pittsburgh, PA, USA). Since this homogenization step is carried out a temperature that is at least 10 °C greater than the melting point of the lipid, the primary product at this stage was a nanoemulsion due to the liquid state of the lipid. At the end of sonication, the mixture was dispersed into 30 mL of an ice-cold surfactant solution maintained in an ice bath. The final mixture was then sonicated at a specific speed for a predetermined time interval (speed and sonication times described in subsequent section) immersed in the ice-bath. This cooling step promoted the formation of the solid lipid nanoparticles. All bulk formulations were stored in the refrigerator at 2–8 °C till further analysis.

2.4. Freeze drying of nanoparticles

In order to evaluate the crystallinity of the quercetin nanoparticles, it was essential to convert the liquid to a dried form. Samples were dried using a freeze drying process in a Usifroid Freeze Dryer (Elancourt, France). Pre-cooling from room temperature to −50 °C was achieved at a cooling rate of 1 °C/min. The sample was then maintained at −50 °C for 1 h, followed by primary and secondary drying using a cooling rate of 1 °C/min. Since the primary purpose of drying the nanoparticles was to obtain a powder for further solid state characterization, no matrix formers were added to the solution prior to freeze drying.

2.5. Characterization of nanoparticles

2.5.1. Particle size determination using photon correlation spectroscopy

The particle size of nanoparticles was measured using a Delsa Nano™ C particle size analyzer (Beckman Coulter, Brea, CA, USA). This instrument uses photon correlation spectroscopy (PCS) to determine the particle size by measuring the rate of fluctuations in laser light intensity scattered by particles as they diffuse through a fluid. The sample (undiluted) was poured into a disposable plastic cuvette, the cuvette manually shaken for about 10 s and then placed inside the sample holder of the particle size analyzer. Once the intensity of the sample was within the permissible range of the instrument, analysis was performed to obtain the particle size and the polydispersity index (PI). All particle size measurements were performed in triplicate using a scattering angle of 90° and at 25 °C.

2.5.2. Zeta potential measurement

In order to quantify the surface charge on the nanoparticles, the zeta potential was measured using a Delsa Nano™ C (Beckman Coulter, Brea, CA, USA). Using electrophoretic light scattering (ELS), the electrophoretic movement of charged particles under an applied electric field is measured. The measured value is then converted into zeta potential using the Helmholtz–Smoluchowski equation that is built into the software. The zeta potential was measured using an appropriately diluted nanoparticle solution with an applied electric field of 16 V/cm. Dilutions were performed with distilled water adjusted to a conductivity of 50 μS/cm by addition of 0.9% (m/v) sodium chloride. Reported values are the mean of three measurements.

2.5.3. Nanoparticle morphology

The morphology of nanoparticles was confirmed using transmission electron microscopy (TEM) using a FEI Tecnai G2 BioTwin transmission electron microscope fitted with a SIS Morada digital camera system (Fei Corporation, Hillsboro, OR, USA). 200 mesh formvar coated copper grids were floated on top of approximately 5–10 μL of liquid sample for around 30 min. The grids were then rinsed with filtered HPLC grade water and allowed to dry. All steps were performed at room temperature. Images were captured at magnifications ranging from 4800× to 150,000×.

2.5.4. X-ray powder diffraction

X-ray powder diffraction analysis was performed on a Bruker D8 Advance (Bruker-AXS, Karlsruhe, Germany) controlled by Diffrac plus XRD commander software. Samples were prepared by spreading freeze dried powder samples on PMMA specimen holder rings from Bruker. All samples were scanned from 2° to 40° 2θ at the rate of 2°/min with 0.02° step size and 0.6 s/step at 40 kV and 40 mA. The divergence and anti-scattering slits were set to 1° and the stage rotated at 30 rpm. Data analysis was performed using "EVA Part 11" version 14.0.0.0.

2.5.5. Drug release studies

Release studies from quercetin lipid nanoparticles were performed using Slide-A-Lyzer® MINI Dialysis devices, 2 mL volume, 10K MWCO (Thermo Scientific, Rockford, IL, USA). The release medium used was a mixture of doubly distilled water and absolute alcohol (65:35%, v/v) (Li et al., 2009). The solubility of quercetin in the release medium was measured at ~0.358 mg/mL, which ensured sufficient sink conditions throughout the study. 2 mL of the respective quercetin formulations were added to the donor compartment of the dialysis device and 44.5 mL of the release medium was added to the receptor compartment. The experiment was carried out at 37 °C and at a stirring speed of 100 rpm. Sampling was carried out at 2, 4, 6, 8, 24 and 30 h. At each sampling time point, 1 mL of receptor medium was withdrawn and replaced with fresh medium. The withdrawn samples were analyzed using the HPLC based method described in Section 2.5.6. The release from each formulation was measured in triplicate.

2.5.6. Detection of quercetin by HPLC

Quercetin concentrations were determined using an Agilent HPLC 1100 (Agilent Technologies Inc., Santa Clara, CA, USA) consisting of a standard quarternary pump, diode array detector, an autosampler and vacuum degasser (Model G1311A) run by Chemstation software version B.03.01. Chromatographic separation was achieved using a Phalanx C_{18}, 250 mm × 4.6 mm, 5 μm column (Higgins Analytical, Mountain View, CA, USA). The mobile phase consisted of a mixture of 80% methanol and 20% water (pH adjusted to 3.72 with glacial acetic acid). An isocratic method with the following parameters was used: injection volume of 20 μL, flow rate of 1.0 mL/min, column temperature of 30 °C and a detection wavelength of 370 nm. The total run time was 8 min. External standards were prepared at the following concentrations in the mobile phase: 0.1, 0.5, 1, 5, 10, 25, 50 and 100 μg/mL. These standards were used to determine the linearity (R^2 = 0.999) and the limit of detection (0.5 μg/mL).

2.5.7. Stability study

The selected lipid nanoparticle variant was placed on stability at 2–8 °C. Physical stability of the sample (determined by particle size measurements) was assessed at 1, 2, 6 and 8 weeks. All reported particle size data is the mean of three separate measurements.

2.5.8. In vitro skin permeation study

2.5.8.1. In vitro permeation study using human skin. In vitro permeation studies (n = 5–6 for each formulation) were carried out over a period of 24 h using vertical Franz diffusion cells (PermeGear, Inc., Hellertown, PA, USA) with a diffusion area of 0.64 cm^2 and a receptor compartment volume of 5.1 mL. Full thickness human skin used in this study was obtained from New York Presbyterian Hospital (New York, NY, USA). The skin was thawed for 30 min and then hydrated by immersing in PBS solution for 60 min at 37 °C prior to the start of each experiment. The skin was then cut into appropriate sized sections and mounted on the Franz diffusion cell, with the stratum corneum facing the donor compartment (where the formulation was applied) and the dermis facing the receptor compartment. The receptor compartment was filled with PBS solution (pH 7.4) containing 1% Tween 20 and maintained at a temperature of 37 ± 0.1 °C and a stirring speed of 600 rpm throughout the course of the experiment. 0.5 mL of formulation (SLN or control) was added to each donor compartment and occluded with Parafilm® to prevent evaporation. For the preliminary experiments, samples were withdrawn at regular intervals from the receptor compartment. At 2, 4, 6, 8 and 24 h, 300 μL of sample was withdrawn from the receptor compartment and replaced by an equal volume of fresh receptor media maintained at 37 °C. The withdrawn samples were stored in the refrigerator prior to HPLC analysis.

2.5.8.2. Extraction of quercetin from human skin. At the end of 24 h, the formulation was carefully removed from the donor compartment using a glass transfer pipette. The surface of the skin was thoroughly washed with distilled water to remove any excess formulation and allowed to dry at ambient temperature. The area of the skin corresponding to the diffusion area of the Franz cell was then punched out, weighed accurately and cut into fine pieces. 1 mL of methanol was added to the skin pieces and homogenized using a Polytron® PT 10-35 homogenizer (Kinematica, Inc., Bohemia, NY, USA). The homogenized material was sonicated for 60 min at 37 °C

using a VWR Ultrasonic B5500A-DTH sonicator (VWR International, LLC, Radnor, PA, USA). After sonication, the samples were centrifuged for 30 min at 4000 rpm using an Allegra™ 6R centrifuge (Beckman Coulter, Brea, CA, USA). The supernatant obtained after centrifugation was collected and analyzed using the HPLC method described in Section 2.5.6, with an increased injection volume of 50 μL.

2.5.9. Statistical analysis

All particle size, zeta potential and *in vitro* release rate measurements were performed in triplicate. Means and standard deviations were calculated using Microsoft® Excel 2010. Mean values were compared using Student's *t*-test, with differences being considered as significant at a level of $p < 0.05$.

3. Results and discussion

3.1. Selection of surfactant system

The new surfaces generated due to particle size reduction during the production of solid lipid nanoparticles leads to an increase in the attractive forces between the particles, which increases the surface tension at the interface and destabilizes the system leading to physical instability. The incorporation of a surfactant in the formulation imparts a repulsive force between the nanoparticles and reduces the surface energy and the surface tension of the system (Tanvir and Qiao, 2012). Hence, the selection of the type and concentration of surfactant is important for the long term physical stability of the nanosystem (Uner et al., 2004).

All classes of surfactants (with respect to charge and molecular weight) have been reported in the literature to stabilize SLN systems. For SLN systems intended for skin delivery, the use of both non-ionic surfactants (Montenegro et al., 2012; Mitri et al., 2011) and ionic surfactants (Shah et al., 2007; Souto et al., 2005) have been reported. In this study, we have screened three non-ionic (Poloxamer 188, Tween 20 and Tween 80) and two anionic (sodium lauryl sulfate and dioctyl sodium sulfosuccinate) surfactants to determine the most suitable systems for further evaluation in SLN formulations. Poloxamer 188 (Freitas and Muller, 1999; Siekmann and Westesen, 1994b), Tween 20 and Tween 80 have been previously used as non-ionic stabilizers for SLN systems (Goppert and Muller, 2005; Lv et al., 2009; Sanna et al., 2007). In general, non-ionic surfactants have been shown to have a minor effect in permeation enhancement across human skin whereas anionic surfactants can have a more pronounced effect (Williams and Barry, 2004). Additionally, micelle forming low molecular weight anionic surfactants such as sodium lauryl sulfate can rapidly re-distribute and cover the new surfaces created during particle size reduction in the homogenization step of generating nanoparticles (Mehnert and Mader, 2001). This justified the inclusion of the two anionic surfactants, sodium lauryl sulfate and dioctyl sodium sulfosuccinate, in the list of surfactants being screened.

The surfactant concentration has a great impact on the particle size distribution and stability of the lipid nanoparticles (Han et al., 2008). The adequate coverage of surfactant at the interface has been reported to influence the stability of SLNs *via* surface-mediated crystal growth (Helgason et al., 2009). Hence, in order to select the optimum surfactant concentration for further evaluation in SLN systems, the surface tension of the surfactants was measured in deionized water in concentrations covering a range of 0.05–5% (w/v). The results are presented in Fig. 1. For the non-ionic surfactants Tween 20 and Tween 80, the surface tension reached a plateau in the concentration range of 2.5–5% (w/v). Poloxamer 188 however showed different results, where it was evident that a plateau in surface tension value had not been attained even at the highest concentration (5%, w/v) evaluated in this study. This can be explained by the higher critical micelle concentration of Poloxamer 188 which has been reported to be 0.48 mM (Kabanov et al., 2002) compared to reported values of 0.06 mM for Tween 20 and 0.012 mM for Tween 80 (le Maire et al., 2000) at 25 °C. For the two anionic surfactants tested, the maximum reduction in surface tension was observed in the range of 1.25–2.5% (w/v) concentrations (Fig. 1).

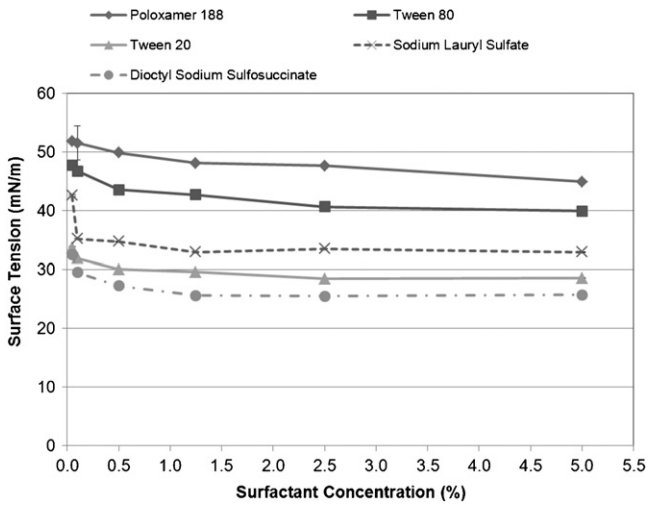

Fig. 1. Surface tension of single surfactant systems determined in water ($n = 3$).

Based on the single surfactant screening data, the three non-ionic surfactants at 2.5% (w/v) concentrations and the two anionic surfactants at 0.1% and 2.5% (w/v) concentrations were further evaluated in combination systems to observe their synergistic effect on surface tension reduction. The data is shown in Table 1. Marked lowering of surface tension was observed for combination surfactant systems. While Poloxamer 188 by itself at 2.5% (w/v) was able to lower the surface tension to 47.63 ± 0.09 mN/m, in combination with 0.1% sodium lauryl sulfate or 0.1% dioctyl sodium sulfosuccinate the surface tension reduced to 28.79 ± 0.04 mN/m and 20.11 ± 0.06 mN/m respectively. Similar results were observed for all the combination systems evaluated (Table 1). Hence some of the combination systems of surfactants were selected for further evaluation in SLN batches as shown in Table 2. Although the anionic surfactants in combination systems showed better effectiveness in reduction of surface tension at 2.5% (w/v) concentrations, the lower levels (0.1%) of these surfactants were selected for further evaluation since anionic surfactants when used in high concentrations have been reported to cause strong barrier disruption and skin irritation (Slotosch et al., 2007).

Solid lipid nanoparticles stabilized with surfactant mixtures have been shown to be more effective in generating nanoparticles with smaller particle sizes and higher storage stability compared to formulations with a single surfactant (Siekmann and Westesen, 1994a). Also, the levels of non-ionic surfactants (2.5%, w/v) selected based on this screening study for further evaluation is in agreement with literature reports where extensive particle aggregation was observed within 24 h for tripalmitin based SLN systems containing less than 2% of Tween 20 (Helgason et al., 2009).

3.2. Effect of formulation variables: selection of solid lipid and optimum surfactant system

Compritol® 888 (glyceryl dibehenate) and Precirol® ATO 5 (glyceryl palmitostearate), which have been extensively used as solid lipids in SLN systems (Mehnert and Mader, 2001) were selected for manufacturing of quercetin solid lipid nanoparticles. Lipids with

Table 1
Surface tension of combination of surfactant systems in water.

Surfactant 1/concentration (%, w/v)	Surfactant 2/concentration (%, w/v)	Surface tension (mN/m), mean ± S.D. ($n = 3$)
Poloxamer 188/2.5%	Sodium lauryl sulfate/0.1%	28.79 ± 0.04
Poloxamer 188/2.5%	Sodium lauryl sulfate/2.5%	26.06 ± 0.07
Poloxamer 188/2.5%	Dicotyl sodium sulfosuccinate/0.1%	20.11 ± 0.06
Poloxamer 188/2.5%	Dicotyl sodium sulfosuccinate/2.5%	18.97 ± 0.01
Tween 20/2.5%	Sodium lauryl sulfate/0.1%	29.40 ± 0.06
Tween 20/2.5%	Sodium lauryl sulfate/2.5%	25.95 ± 0.08
Tween 20/2.5%	Dicotyl sodium sulfosuccinate/0.1%	26.95 ± 0.10
Tween 20/2.5%	Dicotyl sodium sulfosuccinate/2.5%	19.20 ± 0.16
Tween 80/2.5%	Sodium lauryl sulfate/0.1%	27.26 ± 0.01
Tween 80/2.5%	Sodium lauryl sulfate/2.5%	27.91 ± 0.01
Tween 80/2.5%	Dicotyl sodium sulfosuccinate/0.1%	27.13 ± 0.04
Tween 80/2.5%	Dicotyl sodium sulfosuccinate/2.5%	20.39 ± 0.01

Table 2
Composition and initial particle size of batches from the formulation optimization trials.

Batch code	Lipid/ratio (%)	Primary surfactant (%)	Secondary surfactant (%)	D_{50} (nm)	D_{90} (nm)	Acceptable
B1	Compritol® 888/100	Poloxamer 188 (2.5)	DOSS (0.1)	>1000	>1000	No
B2	Compritol® 888/100	Poloxamer 188 (2.5)	SLS (0.1)	354.0 ± 63.3	>1000	No
B3	Compritol® 888/100	Tween 20 (2.5)	DOSS (0.1)	321.0 ± 12.2	643.1 ± 24.0	Yes
B4	Compritol® 888/100	Tween 20 (2.5)	SLS (0.1)	355.8 ± 8.8	756.2 ± 34.0	Yes
B5	Compritol® 888/100	Tween 80 (2.5)	DOSS (0.1)	290.5 ± 9.8	579.2 ± 35.9	Yes
B6	Compritol® 888/100	Tween 80 (2.5)	SLS (0.1)	324.2 ± 11.3	629.4 ± 40.1	Yes
B7	Compritol® 888:Precirol® ATO 5/60:40	Poloxamer 188 (2.5)	DOSS (0.1)	>1000	>1000	No
B8	Compritol® 888:Precirol® ATO 5/60:40	Poloxamer 188 (2.5)	SLS (0.1)	710.4 ± 54.6	>1000	No
B9	Compritol® 888:Precirol® ATO 5/60:40	Tween 20 (2.5)	DOSS (0.1)	384.1 ± 12.1	865.3 ± 50.3	Yes
B10	Compritol® 888:Precirol® ATO 5/60:40	Tween 20 (2.5)	SLS (0.1)	618.4 ± 59.4	>1000	No
B11	Compritol® 888:Precirol® ATO 5/60:40	Tween 80 (2.5)	DOSS (0.1)	343.6 ± 7.8	795.9 ± 48.4	Yes
B12	Compritol® 888:Precirol® ATO 5/60:40	Tween 80 (2.5)	SLS (0.1)	598.6 ± 20.9	>1000	No

relatively low monoglyceride content were selected for evaluation since reports in the literature suggested the generation of unstable SLNs with lipids having high monoglyceride content (Jensen et al., 2010). The batch composition for the formulation optimization trials is shown in Table 2. Two lipid compositions were selected for preparing the nanoparticles, 100% Compritol® 888 and a mixture of Compritol® 888 and Precirol® ATO 5 in the ratio of 60:40. These lipid compositions were selected from preliminary solubility studies of quercetin in lipid mixtures of varying compositions by visually observing the amount of quercetin that could be dissolved in molten lipids (data not shown).

The initial particle size of the SLN batches from the formulation optimization trials is shown in Table 2. For all four batches (B1, B2, B7 and B8) manufactured using Poloxamer 188 as the primary surfactant at 2.5% (w/v) levels, particles in the nanometer range could not be generated irrespective of the solid lipids or the secondary surfactant used. This could be because the amount of Poloxamer 188 used in these batches was not adequate to provide sufficient coverage of the new surfaces generated due to size reduction during the homogenization process. This can be further explained by the redistribution processes of surfactant molecules between particle surfaces, water-solubilized monomers and micelles which have been reported to take a longer time for high molecular weight surfactants such as Poloxamer 188 (Mehnert and Mader, 2001). The inability to generate nanoparticles with 2.5% (w/v) of the non-ionic surfactant Poloxamer 188 is consistent with several literature observations with other non-ionic surfactants (Siekmann and Westesen, 1994a; Schwarz and Mehnert, 1999). Based on literature references, there seems to be no indication of chemical incompatibility between quercetin and Poloxamer (Kakran et al., 2011; Parmar et al., 2011).

Nanoparticles could be successfully generated for batches B3, B4, B5 and B6 manufactured using Compritol® 888 as the solid lipid (based on D_{50} and D_{90} measurements, Table 2). This demonstrated that a combination of a non-ionic surfactant (Tween 20 or Tween 80) at 2.5% (w/v) along with an anionic surfactant (SLS or DOSS) at 0.1% (w/v) levels was adequate to provide sufficient coverage of Compritol® 888 based quercetin nanoparticles and prevent aggregation during production. Batches (B9, B10, B11 and B12) composed of a mixture of solid lipids (3:2 ratio of Compritol® 888:Precirol® ATO 5) did not perform as well as batches composed of Compritol® 888 as the sole lipid with respect to generation of nanoparticles. For batches B9 and B11, although nanoparticles could be generated, D_{90} values in the range of 795–865 nm were obtained. For batches B10 and B12, nanoparticles could not be produced. The possible reason for the inability to generate nanoparticle batches with a mixture of Compritol® 888:Precirol® ATO 5 is discussed in the next paragraph.

Previous studies have attributed the instability of solidified lipid nanoparticles to the tendency of lipids to initially crystallize in the unstable α form due to the lower activation energy followed by transformation to the more ordered β-form (Himawan et al., 2006). Electron microscopy has confirmed that crystals generated with the α structure are more spherical whereas modification to the β-form results in the formation of a platelet-like layered structure (Bunjes et al., 2007). Consequently the surface-to-volume ratio of crystals in the layered β-form is much higher than those crystals in

the spherical α form. Freshly solidified samples of both Compritol® and Precirol® (as would apply to a SLN system) have been shown to exist in a partially amorphous layered structure which tends to slowly crystallize further with time (Hamdani et al., 2003). This layered structure indicates the onset of lipid transformation even in freshly solidified samples. The crystallization of Precirol® is reported to occur rapidly whereas the crystallization of Compritol® is a much more gradual process, often occurring over a period of several months. This difference in the rate of crystallization can be explained by the longer fatty acid chain in Compritol® (C-22) compared to Precirol® (C16–C18) which results in the longer crystallization times for Compritol® (Laine et al., 1988). It is suggested that the lipid nanoparticles composed of mixed lipids (containing 40% Precirol®) underwent a much faster rate of lipid transformation. In the absence of adequate amounts of surfactant, the new surfaces created during lipid transformation could not be fully covered by surfactant molecules leading to physical instability and aggregation of the solid lipid nanoparticles.

The six batches (B3, B4, B5, B6, B9 and B11) for which nanoparticles could be generated were placed on a short term stability study for 1 week at 2–8 °C to observe their aggregation behavior upon storage. Batches composed of mixed lipids (B9 and B11) showed considerable aggregation after 1 week with D_{90} values >1 μm. In comparison, batches composed of only Compritol® (B3, B4, B5 and B6) were found to be relatively stable, with particle size increases of 30–50 nm and 80–120 nm observed for D_{50} and D_{90} values respectively between the initial and 1 week stability samples (Fig. 2). For all batches with Compritol®, the polydispersity index initially and after 1 week was <0.3. This is indicative of a narrow particle size distribution and a monodisperse system. The four batches (B3, B4, B5 and B6) composed of 100% Compritol® as the solid lipid were selected for further evaluation.

3.3. Effect of drug loading

For batches described in Section 3.2, the loading of quercetin (based on the amount of solid lipid) had been maintained at 5%. For the four promising formulations B3, B4, B5 and B6, batches with a higher loading of 10% quercetin were manufactured. Increasing the drug loading to 10% led to a distinct increase in the particle size as shown by the D_{50} and D_{90} values (Fig. 3). Although D_{50} values ≤1 μm were observed for all batches with 10% quercetin loading, the D_{90} values were >1 μm. Batches with 10% drug loading also showed an increase in the polydispersity index to values >0.3, indicating deviation from a monodisperse system. The particle size data indicated that the incorporation of 10% quercetin led to a destabilization of the lipid nanoparticles resulting in aggregation. Similar observations with other Compritol® SLN systems have been reported, in which increasing the loading of tetracaine and etomidate from 5% to 10% led to the formation of a less stable product with an increase in the mean particle size (Schwarz and Mehnert, 1999).

3.4. Selection of optimum formulation

The optimum nanoparticle formulation was selected based on physical stability data and batch reproducibility data (replicates). The physical stability data of formulations B3, B4, B5 and B6 kept for up to 6 weeks at 2–8 °C is shown in Figure 2. After 6 weeks of storage at 2–8 °C, the increase in particle size of all formulations was in the range of 26–155 nm (D_{50}) and 97–349 nm (D_{90}). Throughout this study, close attention was paid to the D_{50} and D_{90} values instead of only the mean particle size since D_{90} values are more indicative of the size of the majority of particles (90%) in the system. All the four formulations could still be classified as nanoparticles, with majority of the particles in the sub-micron range, after 6 weeks of storage at 2–8 °C. The polydispersity index values obtained were as follows: 0.218, 0.220, 0.220 and 0.211 at the initial timepoint, 0.235, 0.241, 0.216 and 0.210 after 1 week at 2–8 °C and 0.227, 0.230, 0.275 and 0.251 after 6 weeks at 2–8 °C for batches B3, B4, B5 and B6 respectively. These polydispersity values of <0.3 indicated a monodisperse system for all batches with a narrow particle size distribution.

All four formulations were re-manufactured to check the robustness of the process to replicate the batches. The smallest difference in particle size (52.4 nm for D_{50} values and 93.7 nm for D_{90} values) was observed for batch B3 which was stabilized with a surfactant system composed of 2.5% Tween 20 and 0.1% DOSS, using a solid lipid matrix of 100% Compritol®. This formulation had also

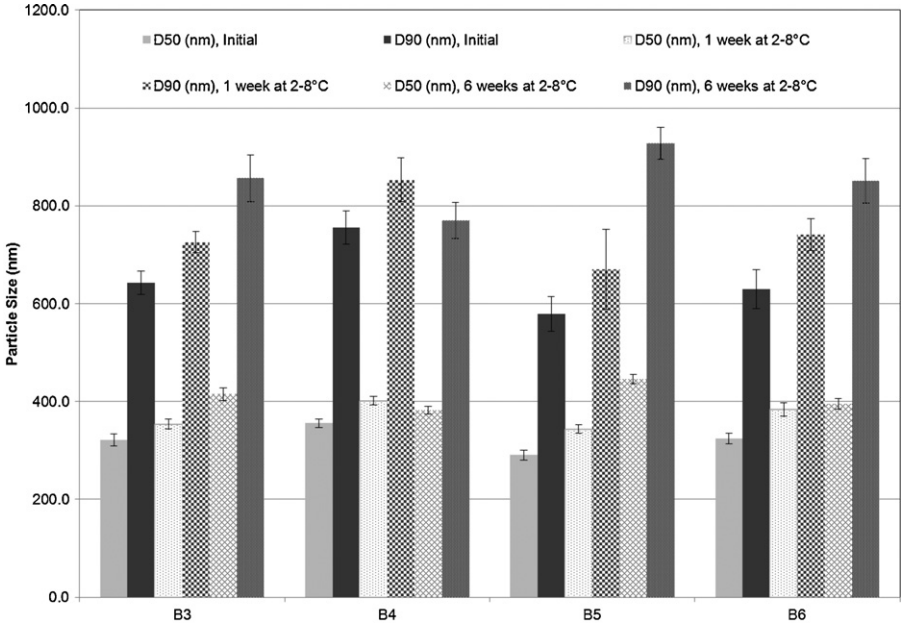

Fig. 2. Selection of optimum formulation: physical stability data ($n = 3$); bars denote standard deviation; bar graphs for each batch (from left to right) denote values of D_{50} at initial, D_{90} at initial, D_{50} after 1 week at 2–8 °C, D_{90} after 1 week at 2–8 °C, D_{50} after 6 weeks at 2–8 °C and D_{90} after 6 weeks at 2–8 °C.

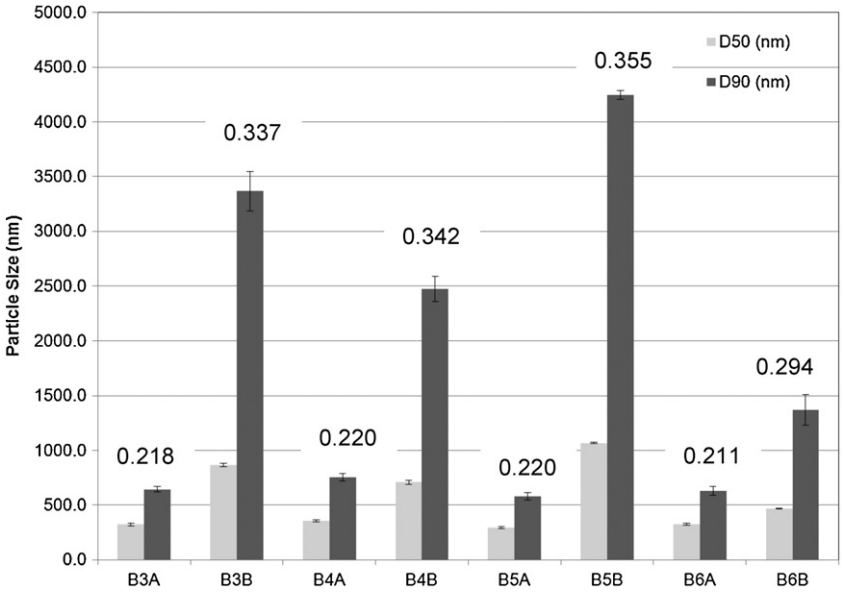

Fig. 3. Effect of drug loading on initial particle size of quercetin lipid nanoparticles ($n = 3$); suffix A and B (on x-axis) denote batches with 5% and 10% loading of quercetin respectively; numbers on graph indicate the polydispersity index (PI) of each batch.

demonstrated adequate physical stability based on particle size data for up to 6 weeks at 2–8 °C and was selected for further optimization of processing parameters.

3.5. Optimization of processing parameters

During the formulation optimization trials described in the previous sections, all batches had been manufactured using a first sonication step of 5 min at 85 °C (homogenization step), followed by a second sonication step of 10 min in an ice bath (sample cooling step to enable lipid crystallization and generation of solid lipid nanoparticles). Once a promising formulation had been selected, optimization of the manufacturing process parameters was carried out. The investigated parameters are specified in Table 3. The study involved evaluation of two levels of the sonication time used during the first step (5 min and 30 min) and two levels of the power setting used during the second sonication step (power setting of 1 and 4). For the first sonication step, the power setting was kept constant at 4 so that sufficient energy could be introduced into the system to break down the micron sized particles. The initial particle size data from the process optimization batches is shown in Table 3. The smallest particle size (based on both D_{50} and D_{90} values) was observed for batches manufactured using a first sonication step of 30 min. This can be explained by the higher input of energy into the system during the longer sonication time resulting in more efficient particle size reduction. Hence this is considered to be a critical parameter of the manufacturing process and a sonication time of 30 min during the first step was selected for future batches. This observation is consistent with another report in the literature, where sonication times greater than 15 min were required to generate nanoparticles using a probe sonication method (Siekmann and Westesen, 1994b). The power level of the second sonication step (setting of 1 against 4) did not appear to affect the formation of nanoparticles based on a comparison of batches B3A3 and B3A4, where all processing parameters except that parameter had been maintained constant. For the second sonication step, the lower power level was selected for subsequent batches to prevent the possible disruption of nanoparticles during the lipid solidification step by using the higher power level resulting in high energy input to the system. Such energy input can cause destabilization of the SLN system by causing damage to the surfactant film covering the particle surface promoting aggregation (Freitas and Muller, 1999).

The measurement of zeta potential is critical to predict the stability of colloidal dispersions upon long term storage (Komatsu et al., 1995). In general, particle aggregation upon storage is less likely to occur for highly charged particles (with high zeta potential values) because the repulsion forces arising from the surface charge can overcome the Van der Waals attractive forces between the particles. Usually an absolute zeta potential value of 20 mV or higher is indicative of a stable system (Gonzalez-Mira et al., 2011). The zeta potential of formulations evaluated during the process optimization study ranged from -32.88 ± 0.86 mV to -35.83 ± 2.11 mV (Table 3) which indicated adequate stabilization of the nanoparticle system. The difference in zeta potential values observed between the four formulations was not found to be statistically different ($p > 0.05$).

3.6. Stability data

The solid lipid nanoparticle batch composed of 5% (w/v) quercetin (relative to the lipid), a surfactant system consisting of 2.5% Tween 20 and 0.1% DOSS in a solid lipid matrix of 100% Compritol® was placed on long term stability at 2–8 °C for up to 8 weeks. At pre-determined time intervals, samples were withdrawn and the particle size was measured to check for any potential aggregation. The polydispersity index values were as follows: 0.245 for the initial sample, 0.294 for the stability sample kept for 2 weeks at 2–8 °C and 0.293 for the stability sample kept for 8 weeks at 2–8 °C. The differences in particle size (both D_{50} and D_{90} values) between the initial and 2 weeks timepoint were found to be statistically significant ($p < 0.05$). However, no statistically significant differences were found between the D_{50} and D_{90} values for samples kept on stability for 2 weeks and 8 weeks ($p > 0.05$). Similar observations have been reported by Mitri et al. (2011), where increase in particle size was observed for up to 7 days after production, beyond which no significant change in particle size was observed between days 7 and 90.

The increase in particle size between the initial and 2 week sample can be attributed to some degree of lipid transformation occurring for the solid lipid (glyceryl dibehenate) used in these nanoparticles. Triglycerides are known to crystallize in three main

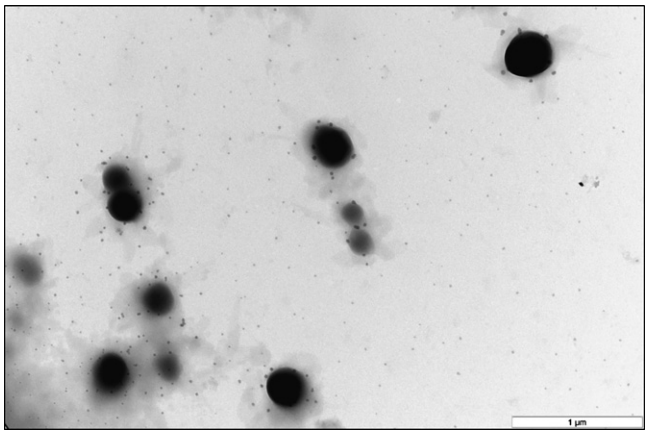

Fig. 4. TEM of quercetin nanoparticles.

polymorphic forms. The unstable α form is initially formed due to its lower activation energy, which has been reported to undergo a monotrophic transformation *via* β′ to β. For mixtures of glycerides, an intermediate form, β_i, between β′ and β has also been suggested. Due to the high content (>50%) of diglycerides, glyceryl dibehenate primarily crystallizes in the β′ modification (Freitas and Muller,1999). Transition from the metastable β′ polymorph to the more stable β_i polymorph occurs over time, which is associated with a certain degree of aggregation. In the case of glyceryl dibehenate, a further transformation of β_i to β has been reported (Jenning et al., 2000b). It is possible that some amount of lipid transformation from the metastable β′ to the more stable β_i occurs between the initial and 2 weeks timepoint for the glyceryl dibehenate based quercetin SLNs, leading to an increase in the particle size. However, the relative stabilization of particle size between 2 weeks and 8 weeks indicates incomplete transformation of the lipid from the β′ to the β_i configuration. This can also be confirmed by the TEM and XRD data which will be discussed in the subsequent sections. This observation is consistent with reports of successful stabilization of the metastable β′ polymorph and control of the β′ to β_i transition by using a mixture of surfactants in the SLN formulation (Jenning et al., 2000b). Also, systems containing non-ionic surfactants have been reported to transform more rapidly into the β form compared to systems containing ionic surfactants (Bunjes et al., 2003). Since a combination system consisting of a non-ionic (Tween 20) and an ionic (DOSS) surfactant has been used to stabilize the quercetin lipid based nanoparticles, it is quite possible that the metastable β′ polymorph of glyceryl dibehenate could be stabilized to a certain extent leading to only partial transformation from the β′ to β_i polymorph.

3.7. Morphology of nanoparticles

Nanoparticle morphology observed using transmission electron microscopy (TEM) showed spherical particles in the nanometer range (Fig. 4). The shape of the particles was consistent with those observed from other quercetin SLN systems evaluated for brain delivery (Dhawan et al., 2011) and for oral delivery (Li et al., 2009). The spherical shape of the particles also supported the hypothesis of partial transformation of glyceryl behenate from the metastable β′ to the more stable β_i configuration since an alteration in particle geometry from a round to a polyhedric form is associated with a complete transformation of glyceryl behenate from β′ to the β_i form (Jenning et al., 2000b).

3.8. XRD data

The XRD data of bulk compritol and the freeze dried SLN formulation is shown in Fig. 5. The diffractogram labeled as A shows the diffraction pattern of neat Compritol® 888 with peaks characteristic of the orthorhombic β′ form of triglycerides (Chapman, 1962). However in the freeze dried SLN formulation (labeled as B), an additional peak is observed at 2θ values between 18° and 20°. This peak has been previously assigned to the β_i polymorph (Jenning et al., 2000b). The XRD data supported the theory of partial transformation of glyceryl dibehenate from the metastable β′ to the more stable β_i configuration in the quercetin SLN formulation.

3.9. Drug release studies

In order to exert a therapeutic effect *in vivo*, it is essential that the active is released from the delivery system at the site of application. Formation of a solid particle matrix is essential to adjust the release profile of a drug from lipid nanoparticles since rapid release within a few seconds has been associated with oil-in-water emulsions (Benita et al., 1986). Depending on the production temperature used, different release profiles from solid lipid nanoparticles have been reported. These include rapid release (100% of tetracaine and etomidate released in less than a minute) from SLN prepared by the

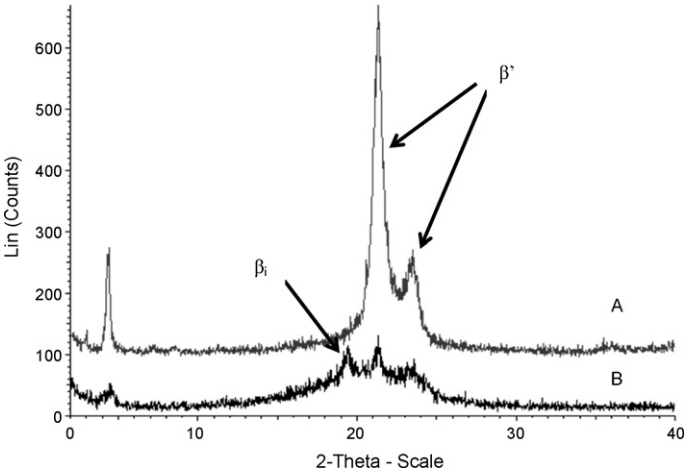

Fig. 5. X-ray diffraction patterns: (A) Compritol® 888 bulk material; (B) freeze dried quercetin nanoparticles.

Table 3
Batch details, initial particle size and zeta potential data for process optimization batches.

Batch code	First sonication step		Second sonication step		Particle size, initial, mean ± S.D. ($n = 3$)			Zeta potential (mV), mean ± S.D. ($n = 3$)
	Time (min)	Power setting	Time (min)	Power setting	D_{50} (nm)	D_{90} (nm)	PI[a]	
B3A1	5	4	10	1	373.4 ± 3.5	736.7 ± 68.6	0.208	−33.35 ± 0.78
B3A2	5	4	10	4	424.0 ± 5.4	903.0 ± 11.1	0.247	−32.88 ± 0.86
B3A3	30	4	10	4	311.5 ± 5.5	646.8 ± 21.9	0.232	−34.24 ± 1.29
B3A4	30	4	10	1	351.6 ± 5.3	697.8 ± 43.1	0.245	−35.83 ± 2.11

[a] Polydispersity index.

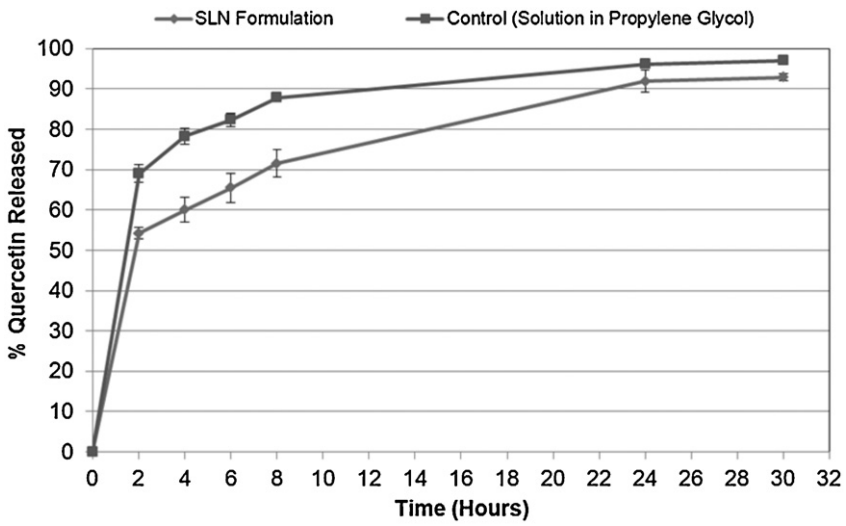

Fig. 6. *In vitro* release profile of quercetin from SLN and propylene glycol solution determined by a dialysis method ($n = 3$).

hot homogenization technique as well as sustained release (prednisolone released over a period of 5 weeks) from SLN prepared by the cold homogenization technique (zur Muhlen et al., 1998). Most researchers have reported a biphasic release profile from solid lipid nanoparticles manufactured using hot homogenization, with an initial burst release followed by prolonged release (Zhang et al., 2010; Rawat et al., 2011). Some of the other factors that influence release profiles are the surfactant type and concentration in the SLN formulation (Muller et al., 2002).

The release of quercetin from the selected SLN formulation was compared using a dialysis based method against a control formulation of quercetin in propylene glycol at the same concentration as in the SLN formulation. The release profiles are shown in Fig. 6. Statistically significant differences ($p < 0.05$) were observed between the rates of release of quercetin from the two formulations at all the time points except at 24 h where the release rate was not statistically significant ($p > 0.05$). The rate of release of quercetin from the SLN formulation was found to be relatively slower compared to the propylene glycol solution, with about 70% released from the SLN formulation compared to 90% released from the propylene glycol solution after 8 h. Equilibrium was attained within 24 h. This was confirmed by running the experiment till 30 h, during which the release rate was observed to reach a plateau between 24 and 30 h indicating attainment of equilibrium. The release profile of quercetin from the SLN formulation is consistent with reported release rates of other actives from Compritol® 888 based nanoparticles containing a similar concentration of surfactant (2.5%) as was used in these quercetin SLN and manufactured using the hot homogenization technique at a similar production temperature (Muller et al., 2002). The initial burst release can be explained by a drug enriched shell model of incorporation of quercetin into SLNs. During the heating step of the hot homogenization process, the solubility of the active compound in the aqueous phase increases, leading to the partitioning of the active compound from the melted lipid droplet to the water phase. During the subsequent cooling step, the lipid matrix starts crystallizing with a relatively high amount of active still concentrated in the aqueous phase. Further cooling leads to supersaturation of the active compound in the aqueous phase that then tries to partition back into the lipid phase. Since a solid core has already started forming, this leaves only the liquid outer shell for the accumulation of active which leads to the formation of a drug enriched shell. This enrichment of drug in the outer shell leads to a short diffusion path of the active, resulting in a burst release profile.

3.10. Topical delivery of quercetin

Skin permeation studies were carried out with the SLN formulation of quercetin, using the corresponding non-homogenized formulation with particle size in the micrometer range as the control. Such studies are also relevant while studying topical drug delivery to make sure that none of the compound appears to permeate transdermally. In our studies, sampling was carried out from the receptor media at 2, 4, 6, 8 and 24 h to determine if there was any transdermal delivery of quercetin. However, no quercetin could be detected in the receptor media, indicating the lack of any transdermal delivery. This observation is consistent with reports from other skin permeation studies of quercetin (Kitagawa et al., 2009; Vicentini et al., 2008), including one study from a chitosan–lecithin based nanoparticle formulation (Tan et al., 2011). The absence of transdermal delivery of quercetin from the lipid nanoparticles can be attributed to the structure and physico-chemical properties of quercetin and the barrier properties of the stratum corneum. One of the reasons contributing to the inability of quercetin to penetrate the skin could be its poor lipophilicity (Montenegro et al., 2007) and rather limited aqueous solubility (Bonina et al., 1996). The chemical structure has also been shown to have a large influence on the percutaneous absorption of quercetin and its related compounds through nude mouse skin (Lin et al., 2012). Lin et al. also demonstrated the stratum corneum to be the principal barrier for skin penetration of quercetin and showed a 4.14 times increase in the flux of quercetin through stratum corneum stripped skin compared to intact skin.

The amount of quercetin quantified in the skin at the end of 24 h is shown in Fig. 7. The SLN formulation showed a higher amount of quercetin retained in the skin at the end of 24 h compared to the control formulation, with the differences being statistically significant ($p < 0.05$). The superior topical delivery of quercetin observed from the lipid based nanosystem compared to the control formulation (containing the same amount of lipid as in the SLN formulation) can be explained by the higher occlusive effect and increased hydration of the stratum corneum commonly associated with lipid nanoparticles (Muller et al., 2007). The increased hydration of the stratum corneum influences the percutaneous absorption of active ingredients contained in the formulation (Zhai and Maibach, 2001). The improved dermal uptake of quercetin from the lipid nanoparticles could also result from an increased contact surface of the active compound with the corneocytes. In general, lipid nanoparticles are not considered to penetrate the horny layer (Schafer-Korting

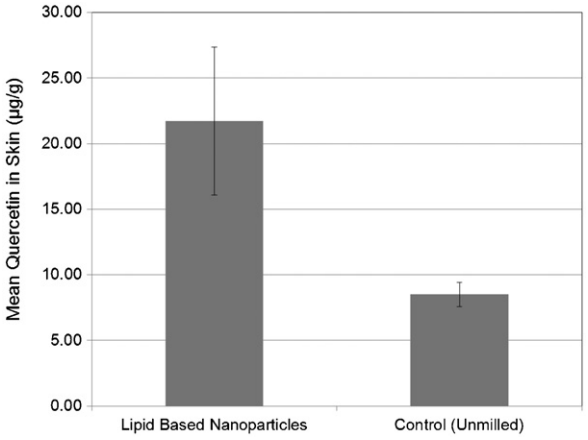

Fig. 7. Topical delivery of quercetin from solid lipid based nanosystem ($n = 5$).

et al., 2007). However, a follicular uptake by the hair follicles has been reported for particulate systems (Lademann et al., 2007). Reduced percutaneous permeation along with increased localization in the skin has also been reported for SLN formulations of diethyltoluamide (Iscan et al., 2005), glucocorticoids (Jensen et al., 2011) and betamethasone 17-valerate (Zhang and Smith, 2011). The amount of quercetin accumulated in the skin from the SLN formulation (2.66 ± 0.81 μg/mL) should be sufficient to exert an adequate anti-oxidant activity against the reactive oxygen species. This is based on a SC_{50} value (concentration to achieve 50% of free radical scavenging activity) of 1.59 ± 0.6 μg/mL reported for a quercetin nanoparticle system (Wu et al., 2008).

Since this was a preliminary formulation screening study, *in vivo* testing which is typically complex and more expensive, was considered out of scope for this study. However, some form of *in vivo* testing would need to be conducted in future to demonstrate the utility of the delivery system for consideration in clinical applications.

4. Conclusion

Surface tension measurements of single surfactants (both non-ionic and ionic) and combinations thereof were carried out to identify systems with the highest surface tension lowering ability. Optimization of formulation and process variables led to the identification of a promising variant composed of 5% quercetin, 2.5% Tween 20 (non-ionic surfactant) and 0.1% DOSS (ionic surfactant), using a solid lipid matrix of 100% Compritol® 888 (glyceryl behenate) and manufactured using probe sonication. The optimized formulation had a zeta potential of -35.83 ± 2.11 mV and demonstrated good physical stability for up to 8 weeks at 2–8 °C. Slight increase in particle size was observed between the initial and 2 week stability samples which was attributed to some degree of lipid transformation of the solid lipid. The onset of lipid transformation was confirmed from the morphology of the nanoparticles visualized using TEM and also from XRD patterns comparing neat Compritol® 888 to freeze dried SLNs. *In vitro* release studies showed an initial burst release followed by prolonged release for up to 24 h from the SLN formulation. Higher amounts of quercetin were found to be localized within the skin compared to a control formulation containing particles in the micrometer range. This study demonstrated the feasibility of topical delivery of quercetin from a solvent-free solid lipid based nanosystem manufactured using probe sonication. Future studies will focus on the evaluation of high pressure homogenization, a scalable manufacturing process, for manufacturing the quercetin loaded SLN systems.

Acknowledgements

The authors would like to acknowledge Reena Nadpara and Marina Botrous for providing assistance during batch manufacturing, Danielle Lazarra for assistance with the skin permeation studies, Karen Killary for the TEM images and Marilyn Alvine for the XRD measurements.

References

Afanas'ev, I.B., Dorozhko, A.I., Brodskii, A.V., Kostyuk, V.A., Potapovitch, A.I., 1989. Chelating and free radical scavenging mechanisms of inhibitory action of rutin and quercetin in lipid peroxidation. Biochem. Pharmacol. 38, 1763–1769.
Azuma, K., Ippoushi, K., Ito, H., Higashio, H., Terao, J., 2002. Combination of lipids and emulsifiers enhances the absorption of orally administered quercetin in rats. J. Agric. Food Chem. 50, 1706–1712.
Benita, S., Friedman, D., Weinstock, M., 1986. Pharmacological evaluation of an injectable prolonged release emulsion of physostigmine in rabbits. J. Pharm. Pharmacol. 38, 653–658.
Bonina, F., Lanza, M., Montenegro, L., Puglisi, C., Tomaino, A., Trombetta, D., Castelli, F., Saija, A., 1996. Flavonoids as potential protective agents against photo-oxidative skin damage. Int. J. Pharm. 145, 87–94.
Bors, W., Heller, W., Michel, C., Saran, M., 1990. Flavonoids as antioxidants: determination of radical-scavenging efficiencies. Methods Enzymol. 186, 343–355.
Bors, W., Michel, C., Saran, M., 1994. Flavonoid antioxidants: rate constants for reactions with oxygen radicals. Methods Enzymol. 234, 420–429.
Bunjes, H., Koch, M.H., Westesen, K., 2003. Influence of emulsifiers on the crystallization of solid lipid nanoparticles. J. Pharm. Sci. 92, 1509–1520.
Bunjes, H., Steiniger, F., Richter, W., 2007. Visualizing the structure of triglyceride nanoparticles in different crystal modifications. Langmuir 23, 4005–4011.
Cao, G., Sofic, E., Prior, R.L., 1997. Antioxidant and prooxidant behavior of flavonoids: structure–activity relationships. Free Radic. Biol. Med. 22, 749–760.
Casagrande, R., Georgetti, S.R., Verri Jr., W.A., Dorta, D.J., dos Santos, A.C., Fonseca, M.J., 2006. Protective effect of topical formulations containing quercetin against UVB-induced oxidative stress in hairless mice. J. Photochem. Photobiol. B 84, 21–27.
Castro, G.A., Coelho, A.L., Oliveira, C.A., Mahecha, G.A., Orefice, R.L., Ferreira, L.A., 2009. Formation of ion pairing as an alternative to improve encapsulation and stability and to reduce skin irritation of retinoic acid loaded in solid lipid nanoparticles. Int. J. Pharm. 381, 77–83.
Censi, R., Martena, V., Hoti, E., Malaj, L., Di, M.P., 2012. Permeation and skin retention of quercetin from microemulsions containing Transcutol® P. Drug Dev. Ind. Pharm. 38, 1128–1133.
Cevc, G., 2004. Lipid vesicles and other colloids as drug carriers on the skin. Adv. Drug Deliv. Rev. 56, 675–711.
Chapman, D., 1962. The polymorphism of glycerides. Chem. Rev. 62, 433–456.
Chen-yu, G., Chun-fen, Y., Qi-lu, L., Qi, T., Yan-wei, X., Wei-na, L., Guang-xi, Z., 2012. Development of a quercetin-loaded nanostructured lipid carrier formulation for topical delivery. Int. J. Pharm. 430, 292–298.
Delmas, T., Couffin, A.C., Bayle, P.A., Crecy, F.d., Neumann, E., Vinet, F., Bardet, M., Bibette, J., Texier, I., 2011. Preparation and characterization of highly stable lipid nanoparticles with amorphous core of tuneable viscosity. J. Colloid Interface Sci. 360, 471–481.
Dhawan, S., Kapil, R., Singh, B., 2011. Formulation development and systematic optimization of solid lipid nanoparticles of quercetin for improved brain delivery. J. Pharm. Pharmacol. 63, 342–351.
Dingler, A., Blum, R.P., Niehus, H., Muller, R.H., Gohla, S., 1999. Solid lipid nanoparticles (SLN/Lipopearls) – a pharmaceutical and cosmetic carrier for the application of vitamin E in dermal products. J. Microencapsul. 16, 751–767.
Erden Inal, M., Kahraman, A., Koken, T., 2001. Beneficial effects of quercetin on oxidative stress induced by ultraviolet A. Clin. Exp. Dermatol. 26, 536–539.
Freitas, C., Muller, R.H., 1999. Correlation between long-term stability of solid lipid nanoparticles (SLN) and crystallinity of the lipid phase. Eur. J. Pharm. Biopharm. 47, 125–132.
Gonzalez, S., Fernandez-Lorente, M., Gilaberte-Calzada, Y., 2008. The latest on skin photoprotection. Clin. Dermatol. 26, 614–626.
Gonzalez-Mira, E., Nikolic, S., Garcia, M.L., Egea, M.A., Souto, E.B., Calpena, A.C., 2011. Potential use of nanostructured lipid carriers for topical delivery of flurbiprofen. J. Pharm. Sci. 100, 242–251.
Goppert, T.M., Muller, R.H., 2005. Polysorbate-stabilized solid lipid nanoparticles as colloidal carriers for intravenous targeting of drugs to the brain: comparison of plasma protein adsorption patterns. J. Drug Target. 13, 179–187.
Hamdani, J., Moes, A.J., Amighi, K., 2003. Physical and thermal characterisation of Precirol and Compritol as lipophilic glycerides used for the preparation of controlled-release matrix pellets. Int. J. Pharm. 260, 47–57.
Han, F., Li, S., Yin, R., Liu, H., Xu, L., 2008. Effect of surfactants on the formation and characterization of a new type of colloidal drug delivery system: nanostructured lipid carriers. Colloids Surf. A: Physicochem. Eng. Aspects 315, 210–216.
Helgason, T., Awad, T.S., Kristbergsson, K., McClements, D.J., Weiss, J., 2009. Effect of surfactant surface coverage on formation of solid lipid nanoparticles (SLN). J. Colloid Interface Sci. 334, 75–81.
Himawan, C., Starov, V.M., Stapley, A.G., 2006. Thermodynamic and kinetic aspects of fat crystallization. Adv. Colloid Interface Sci. 122, 3–33.

Iscan, Y., Wissing, S.A., Hekimoglu, S., Muller, R.H., 2005. Solid lipid nanoparticles (SLN) for topical drug delivery: incorporation of the lipophilic drugs N,N-diethyl-m-toluamide and vitamin K. Pharmazie 60, 905–909.
Jenning, V., Gysler, A., Schafer-Korting, M., Gohla, S.H., 2000a. Vitamin A loaded solid lipid nanoparticles for topical use: occlusive properties and drug targeting to the upper skin. Eur. J. Pharm. Biopharm. 49, 211–218.
Jenning, V., Schafer-Korting, M., Gohla, S., 2000b. Vitamin A-loaded solid lipid nanoparticles for topical use: drug release properties. J. Control. Release 66, 115–126.
Jensen, L.B., Magnussson, E., Gunnarsson, L., Vermehren, C., Nielsen, H.M., Petersson, K., 2010. Corticosteroid solubility and lipid polarity control release from solid lipid nanoparticles. Int. J. Pharm. 390, 53–60.
Jensen, L.B., Petersson, K., Nielsen, H.M., 2011. In vitro penetration properties of solid lipid nanoparticles in intact and barrier-impaired skin. Eur. J. Pharm. Biopharm. 79, 68–75.
Kabanov, A.V., Batrakova, E.V., Alakhov, V.Y., 2002. Pluronic block copolymers as novel polymer therapeutics for drug and gene delivery. J. Control Release 82, 189–212.
Kakran, M., Sahoo, N.G., Li, L., 2011. Dissolution enhancement of quercetin through nanofabrication, complexation, and solid dispersion. Colloids Surf. B: Biointerfaces 88, 121–130.
Kitagawa, S., Tanaka, Y., Tanaka, M., Endo, K., Yoshii, A., 2009. Enhanced skin delivery of quercetin by microemulsion. J. Pharm. Pharmacol. 61, 855–860.
Komatsu, H., Kitajima, A., Okada, S., 1995. Pharmaceutical characterization of commercially available intravenous fat emulsions: estimation of average particle size, size distribution and surface potential using photon correlation spectroscopy. Chem. Pharm. Bull. (Tokyo) 43, 1412–1415.
Lademann, J., Richter, H., Teichmann, A., Otberg, N., Blume-Peytavi, U., Luengo, J., Weiss, B., Schaefer, U.F., Lehr, C.M., Wepf, R., Sterry, W., 2007. Nanoparticles – an efficient carrier for drug delivery into the hair follicles. Eur. J. Pharm. Biopharm. 66, 159–164.
Laine, E., Auramo, P., Kahela, P., 1988. On the structural behaviour of triglycerides with time. Int. J. Pharm. 43, 241–247.
Laughton, M.J., Evans, P.J., Moroney, M.A., Hoult, J.R., Halliwell, B., 1991. Inhibition of mammalian 5-lipoxygenase and cyclo-oxygenase by flavonoids and phenolic dietary additives. Relationship to antioxidant activity and to iron ion-reducing ability. Biochem. Pharmacol. 42, 1673–1681.
le Maire, M., Champeil, P., Moller, J.V., 2000. Interaction of membrane proteins and lipids with solubilizing detergents. Biochim. Biophys. Acta 1508, 86–111.
Li, H., Zhao, X., Ma, Y., Zhai, G., Li, L., Lou, H., 2009. Enhancement of gastrointestinal absorption of quercetin by solid lipid nanoparticles. J. Control Release 133, 238–244.
Lin, C.F., Leu, Y.L., Al-Suwayeh, S.A., Ku, M.C., Hwang, T.L., Fang, J.Y., 2012. Anti-inflammatory activity and percutaneous absorption of quercetin and its polymethoxylated compound and glycosides: the relationships to chemical structures. Eur. J. Pharm. Sci. 47, 857–864.
Lv, Q., Yu, A., Xi, Y., Li, H., Song, Z., Cui, J., Cao, F., Zhai, G., 2009. Development and evaluation of penciclovir-loaded solid lipid nanoparticles for topical delivery. Int. J. Pharm. 372, 191–198.
Mehnert, W., Mader, K., 2001. Solid lipid nanoparticles: production, characterization and applications. Adv. Drug Deliv. Rev. 47, 165–196.
Mei, Z., Chen, H., Weng, T., Yang, Y., Yang, X., 2003. Solid lipid nanoparticle and microemulsion for topical delivery of triptolide. Eur. J. Pharm. Biopharm. 56, 189–196.
Mitri, K., Shegokar, R., Gohla, S., Anselmi, C., Muller, R.H., 2011. Lipid nanocarriers for dermal delivery of lutein: preparation, characterization, stability and performance. Int. J. Pharm. 414, 267–275.
Montenegro, L., Carbone, C., Maniscalco, C., Lambusta, D., Nicolosi, G., Ventura, C.A., Puglisi, G., 2007. In vitro evaluation of quercetin-3-O-acyl esters as topical prodrugs. Int. J. Pharm. 336, 257–262.
Montenegro, L., Sinico, C., Castangia, I., Carbone, C., Puglisi, G., 2012. Idebenone-loaded solid lipid nanoparticles for drug delivery to the skin: in vitro evaluation. Int. J. Pharm. 434, 169–174.
Morel, I., Lescoat, G., Cogrel, P., Sergent, O., Pasdeloup, N., Brissot, P., Cillard, P., Cillard, J., 1993. Antioxidant and iron-chelating activities of the flavonoids catechin, quercetin and diosmetin on iron-loaded rat hepatocyte cultures. Biochem. Pharmacol. 45, 13–19.
Muller, R.H., Petersen, R.D., Hommoss, A., Pardeike, J., 2007. Nanostructured lipid carriers (NLC) in cosmetic dermal products. Adv. Drug Deliv. Rev. 59, 522–530.
Muller, R.H., Radtke, M., Wissing, S.A., 2002. Solid lipid nanoparticles (SLN) and nanostructured lipid carriers (NLC) in cosmetic and dermatological preparations. Adv. Drug Deliv. Rev. 54 (Suppl. 1), S131L S155.
Olivella, M.S., Lhez, L., Pappano, N.B., Debattista, N.B., 2007. Effects of dimethylformamide and L-menthol permeation enhancers on transdermal delivery of quercetin. Pharm. Dev. Technol. 12, 481–484.
Parmar, A., Singh, K., Bahadur, A., Marangoni, G., Bahadur, P., 2011. Interaction and solubilization of some phenolic antioxidants in Pluronic® micelles. Colloids Surf. B: Biointerfaces 86, 319–326.
Rawat, M.K., Jain, A., Singh, S., 2011. Studies on binary lipid matrix based solid lipid nanoparticles of repaglinide: in vitro and in vivo evaluation. J. Pharm. Sci. 100, 2366–2378.
Rothwell, J.A., Day, A.J., Morgan, M.R., 2005. Experimental determination of octanol–water partition coefficients of quercetin and related flavonoids. J. Agric. Food Chem. 53, 4355–4360.
Sanna, V., Gavini, E., Cossu, M., Rassu, G., Giunchedi, P., 2007. Solid lipid nanoparticles (SLN) as carriers for the topical delivery of econazole nitrate: in-vitro characterization, ex-vivo and in-vivo studies. J. Pharm. Pharmacol. 59, 1057–1064.
Schafer-Korting, M., Mehnert, W., Korting, H.C., 2007. Lipid nanoparticles for improved topical application of drugs for skin diseases. Adv. Drug Deliv. Rev. 59, 427–443.
Schwarz, C., Mehnert, W., 1999. Solid lipid nanoparticles (SLN) for controlled drug delivery. II. Drug incorporation and physicochemical characterization. J. Microencapsul. 16, 205–213.
Semmler, A., Kohler, H.H., 1999. Surface properties of alkylpyridinium chlorides and the applicability of the pendant drop technique. J. Colloid Interface Sci. 218, 137–144.
Shah, K.A., Date, A.A., Joshi, M.D., Patravale, V.B., 2007. Solid lipid nanoparticles (SLN) of tretinoin: potential in topical delivery. Int. J. Pharm. 345, 163–171.
Siekmann, B., Westesen, K., 1994a. Melt-homogenized solid lipid nanoparticles stabilized by the nonionic surfactant tyloxapol. I. Preparation and particle size determination. Pharm. Pharmacol. Lett. 3, 194–197.
Siekmann, B., Westesen, K., 1994b. Thermoanalysis of the recrystallization process of melt-homogenized glyceride nanoparticles. Colloids Surf. B: Biointerfaces 3, 159–175.
Sim, G.S., Lee, B.C., Cho, H.S., Lee, J.W., Kim, J.H., Lee, D.H., Kim, J.H., Pyo, H.B., Moon, D.C., Oh, K.W., Yun, Y.P., Hong, J.T., 2007. Structure activity relationship of antioxidative property of flavonoids and inhibitory effect on matrix metalloproteinase activity in UVA-irradiated human dermal fibroblast. Arch. Pharm. Res. 30, 290–298.
Slotosch, C.M., Kampf, G., Loffler, H., 2007. Effects of disinfectants and detergents on skin irritation. Contact Dermatitis 57, 235–241.
Souto, E.B., Muller, R.H., Gohla, S., 2005. A novel approach based on lipid nanoparticles (SLN®) for topical delivery of α-lipoic acid. J. Microencapsul. 22, 581–592.
Souto, E.B., Wissing, S.A., Barbosa, C.M., Muller, R.H., 2004. Development of a controlled release formulation based on SLN and NLC for topical clotrimazole delivery. Int. J. Pharm. 278, 71–77.
Tan, Q., Liu, W., Guo, C., Zhai, G., 2011. Preparation and evaluation of quercetin-loaded lecithin–chitosan nanoparticles for topical delivery. Int. J. Nanomed. 6, 1621–1630.
Tanvir, S., Qiao, L., 2012. Surface tension of nanofluid-type fuels containing suspended nanomaterials. Nanoscale Res. Lett. 7, 226.
Uner, M., Wissing, S.A., Yener, G., Muller, R.H., 2004. Influence of surfactants on the physical stability of solid lipid nanoparticle (SLN) formulations. Pharmazie 59, 331–332.
Vicentini, F.T., Simi, T.R., Del Ciampo, J.O., Wolga, N.O., Pitol, D.L., Iyomasa, M.M., Bentley, M.V., Fonseca, M.J., 2008. Quercetin in w/o microemulsion: in vitro and in vivo skin penetration and efficacy against UVB-induced skin damages evaluated in vivo. Eur. J. Pharm. Biopharm. 69, 948–957.
Williams, A.C., Barry, B.W., 2004. Penetration enhancers. Adv. Drug Deliv. Rev. 56, 603–618.
Wissing, S., Lippacher, A., Muller, R., 2001. Investigations on the occlusive properties of solid lipid nanoparticles (SLN). J. Cosmet. Sci. 52, 313–324.
Wu, T.H., Yen, F.L., Lin, L.T., Tsai, T.R., Lin, C.C., Cham, T.M., 2008. Preparation, physicochemical characterization, and antioxidant effects of quercetin nanoparticles. Int. J. Pharm. 346, 160–168.
Zhai, H., Maibach, H.I., 2001. Effects of skin occlusion on percutaneous absorption: an overview. Skin Pharmacol. Appl. Skin Physiol. 14, 1–10.
Zhang, J., Smith, E., 2011. Percutaneous permeation of betamethasone 17-valerate incorporated in lipid nanoparticles. J. Pharm. Sci. 100, 896–903.
Zhang, X., Liu, J., Qiao, H., Liu, H., Ni, J., Zhang, W., Shi, Y., 2010. Formulation optimization of dihydroartemisinin nanostructured lipid carrier using response surface methodology. Powder Technol. 197, 120–128.
zur Muhlen, A., Schwarz, C., Mehnert, W., 1998. Solid lipid nanoparticles (SLN) for controlled drug delivery – drug release and release mechanism. Eur. J. Pharm. Biopharm. 45, 149–155.